Organic Electronics 115 (2023) 106760

Contents lists available at ScienceDirect

Organic Electronics

journal homepage: www.elsevier.com/locate/orgel

Modelling the effect of dipole ordering on charge-carrier mobility in organic semiconductors

Thomas Pope [a], Yvelin Giret [a], Miriam Fsadni [a], Pablo Docampo [b], Chris Groves [c], Thomas J. Penfold [a,*]

[a] Chemistry, School of Natural and Environmental Sciences, Newcastle University, Newcastle upon Tyne, NE1 7RU, UK
[b] School of Chemistry, Joseph Black Building, University of Glasgow, Glasgow, UK
[c] Department of Engineering, University of Durham, Durham, DH1 3LE, UK

ARTICLE INFO

Keywords:
Organic semiconductors
Kinetic Monte Carlo
Hole mobility
Dipole moment
Ordering

ABSTRACT

The hopping mobility in organic semiconductors is strongly influenced by the correlated on-site noise — *i.e.* the dipole–dipole interaction between neighbouring molecules. In this paper, we use Kinetic Monte Carlo (KMC) to study the effect of dipole moment and structural order on the hole mobility of organic molecular semiconductors. While the effect on the charge mobility of the dipole–dipole interactions can be approximately reproduced by a global Gaussian disorder model, our present results show that there are non-trivial local effects that are not incorporated into such an approach. The dipole–dipole interactions give rise to large energy barriers that restrict charged particles to smaller and smaller regions as the dipole magnitude increases. While this effect can only reduce the mobility in any given system, we note that if the dipoles self-organize, potentially driven by the dipole moment itself or by an increase in packing density, the negative effect on the mobility can be reduced.

1. Introduction

The discovery of electroluminescence in organic semiconductors has been the driving force for intense research efforts to exploit these materials in applications for energy conversion. Organic molecular semiconductors are now an important class of materials whose applications range include OLED (Organic Light Emitting Diode) displays [1], OPV (Organic Photo-Voltaic) devices [2], OFETs (Organic Field Effect Transistors) [3], and solar cells [4,5]. One of the key limiting factors of these materials is their low charge carrier mobility when compared to inorganic materials. Understanding and improving the charge carrier transport characteristics of these materials is a core focus of research in this field.

In many small molecule organic semiconductors, electron or hole polarons traverse the material by a thermally activated hopping process. The factors that influence the polaron mobility can either be directly molecular in origin (*e.g.* dipole moment) or indirectly (*e.g.* molecular orientation) [6,7]. While separated, the link between direct and indirect influences on polaron mobility is crucial as molecular orientation in thin films strongly influences the electrical and optical properties of devices. Although the detailed mechanism for the ordering of molecules in thin films remains unclear, contributing molecular level factors include shape, dipole and van der Waals interactions [8].

For hole mobility, which is the focus of the present work, Young et al. [9–12] reported that mobility decreased as the dipole increased. These measurements were broadly explained using a Gaussian disorder model [13]. Here, the molecular dipoles are assumed to be randomly oriented so that their contribution to the energetic landscape of the system can be understood by a Gaussian distribution whose width depends on the dipole magnitude [14,15]. While the exact shape of the distribution is still a matter of debate, the general trend shows that larger dipoles increase the energetic disorder of the system and decrease mobility, consistent with trends observed experimentally [8].

While dipole moment increases the energetic disorder, it may also provide a force to drive an increase in structural order in the film. Indeed, Baldo et al. [16] reported that the fluorescence spectrum of polar molecules may shift due to the formation of ordered domains within an otherwise amorphous film and assigned this effect to strong intermolecular dipole–dipole interactions. In addition, they demonstrated that local ordering in these domains can have a significant effect on the width of the electronic density of states, which is principally due to dipolar disorder [17–19]. The study of the dipole moment in the growth of films has primarily focused upon vapour deposited films [20–22], including ultrastable glasses [23–25]. Here the key aspect is the dynamics of the molecules at the vacuum and vapour interfaces,

* Corresponding author.
E-mail addresses: thomas.pope2@newcastle.ac.uk (T. Pope), tom.penfold@newcastle.ac.uk (T.J. Penfold).

https://doi.org/10.1016/j.orgel.2023.106760
Received 23 August 2022; Received in revised form 11 January 2023; Accepted 29 January 2023
Available online 1 February 2023

which has been used to describe the formation of surface potentials (SP) [26], arising from preferential orientation of polar molecules during the deposition. Recent simulations have reported that the electrostatic interaction between the dipole moments of the molecules limits the SP strength and identify short-range van der Waals interactions between the molecule and the surface during deposition as the driving force behind the anisotropic orientation [27]. However, they are also likely to play a role in solution-processed films where dynamics at the liquid–vapour interface are important for nucleation, *i.e.* initial aggregation and subsequent formation of an amorphous solid and interactions play a key role here as described in refs [28,29].

Given the aforementioned discussion on the influence of molecular dipole moment on the hole mobility, it is important to note that recently, Petrus et al. introduced a series of materials [30,31] exhibiting mobilities comparable to the state-of-the-art hole transporting material, spiro-OMeTAD, but exhibiting a key feature of a large dipole moment (> 8D). They proposed that this dipole, combined with the amide-bond facilitated hydrogen bonding, is anticipated to enable close molecular packing facilitating the high mobility, EDOT-Amide-TPA; 3.9×10^{-5} $cm^2V^{-1}s^{-1}$ compared to spiro-OMeTAD 4.0×10^{-5} $cm^2V^{-1}s^{-1}$. This raises a key question: *Is the mobility good because of the large dipole moment or despite the large dipole moment?* Consequently, in this paper we use Kinetic Monte Carlo (KMC) to study the effect of dipole ordering on the hole mobility of organic molecular semiconductors. We observe that the presence of significant dipole–dipole interactions creates an energetically unfavourable environment for charge transport. Despite this, our analysis demonstrates non-trivial behaviour; as the dipole moment increases, so does the influence of local effects, producing localized routes for the charges through the thin film.

2. Theory

Charge transport in organic semiconductor systems occurs via thermally assisted hopping events. In systems with an uncorrelated site-energy disorder, the charge-carrier mobility depends on the system temperature and the applied electric field [32,33] as well as the charge-carrier density [34]. Similar behaviour has been observed for organic semiconductor arrays with correlated site-energy disorder [35]. In this case, assuming the dipoles are randomly orientated, the effect of correlated noise on site-energy disorder can be mapped onto an uncorrelated energy distribution randomly drawn from a Gaussian density of states. The width of this density of states is linearly related to the magnitude of the dipole moment and can only increase as the dipole moment is increased. Because of this, understanding the effect of the dipole by assuming the dipoles have a random orientation is insufficient to describe systems with a high dipole moment and high carrier mobility, such as EDOT-Amide-TPA [30,31]. Indeed, in cases where the intermolecular couplings are comparable to the disorder, the charge carriers are delocalized across multiple sites [36], and the strict localization of traditional KMC methods becomes limiting. In this respect, it is useful to think of the organic semiconductor arrays as existing on a spectrum between highly ordered systems, that are well understood by coherent transport methods, and highly localized systems that are well understood by incoherent transport methods. To this end, we introduce a model for semi-ordered dipole moments in KMC simulations in the following.

For a given configuration, each charged particle can hop to a site within a set radius ($\sqrt{3}L$, where L is the spacing of the cubic grid points) of its origin site and, for a hopping event from site **i** to site **j**, there is an associated change in energy for the system, $\Delta E_{\mathbf{ij}}$. Given this change in energy, a Miller–Abrahams rate is calculated,

$$k_{\mathbf{ij}} = \omega_0 e^{-2\gamma\left|\mathbf{R_{ij}}\right|} \times \begin{cases} e^{-\Delta E_{\mathbf{ij}}/k_B T} & \Delta E_{\mathbf{ij}} > 0 \\ 1 & \Delta E_{\mathbf{ij}} \leq 0, \end{cases} \tag{1}$$

where $\mathbf{R}_{ij}$ is the spacial vector between sites **i** and **j**, γ is the inverse charge localization and ω_0 is the hopping attempt frequency of the hole. This and all subsequent equations are given in atomic units. All parameters used are given in Section 3.

The change in energy for the system is given by,

$$\Delta E_{\mathbf{ij}} = \left(E_{\mathbf{i}}^{\mathrm{corr}} + E_{\mathbf{i}}^{\mathrm{coul}}\right) - \left(E_{\mathbf{j}}^{\mathrm{corr}} + E_{\mathbf{j}}^{\mathrm{coul}}\right) + \Delta E_{\mathrm{field}}, \tag{2}$$

where $\Delta E_{\mathrm{field}}$ is the change in energy due to the external electric field, $E_{\mathbf{i}}^{\mathrm{coul}}$ is the coulomb energy for a charged particle on site **i** and $E_{\mathbf{i}}^{\mathrm{corr}}$ is the correlated disorder at site **i**. Here, we omit the uncorrelated energetic disorder resulting from conformational freedom of the polymer so that the effect of the dipole ordering can be unambiguously studied.

The coulomb term, resulting from electrostatic interaction between a charged particle and all other charged particles in the system, is given by,

$$E_{\mathbf{a}}^{\mathrm{coul}} = \frac{1}{\epsilon_r} \sum_{\substack{b\neq a \\ b=\mathrm{occupied}}} \frac{1}{\left|\mathbf{R_{ab}}\right|}, \tag{3}$$

where ϵ_r is the relative permittivity of the medium.

The correlated disorder term at site **i**, corresponding to the electrostatic energy resulting from the permanent dipoles, $\mathbf{d}_j$, of the adjacent sites is given by,

$$E_{\mathbf{a}}^{\mathrm{corr}} = -\frac{1}{\epsilon_r} \sum_{b\neq a} \frac{\mathbf{d_b}\cdot\mathbf{R_{ab}}}{\left|\mathbf{R_{ab}}\right|^3}. \tag{4}$$

Several factors can determine the dipole orientation. Firstly, the electrostatic interactions of the dipole would be minimized if all the dipoles orient in a corrugated configuration, where each dipole is pointing in the opposite direction to its neighbours. This configuration is unlikely, however, due to the other factors. In devices, the conformation of the molecules will change due to thermal noise, as will their orientation. Depending on the specific nature of the molecules, there may also be steric restrictions on the allowed configurations. The latter terms are expected to dominate in amorphous organic semiconducting devices, although the exact balance will be system specific.

To randomize the dipole directions, we select two random numbers uniformly distributed between 0 and 1, r_φ and r_ϕ. These are then used to define the two rotational degrees of freedom, the azimuthal angle $\cos\phi = (2r_\phi - 1)$ and the polar angle, $\varphi = 2\pi(1-\alpha)r_\varphi$, here α is an order parameter, which is used to restrict the freedom of the dipole moments and simulate the effect of energetically favourable dipole configurations. This parameter can vary to simulate an entirely disordered system, $\alpha = 0$, to a system with rigorous antiferromagnetic dipole stacking, $\alpha = 1$ (that is, for each site every neighbouring site is given a dipole vector pointing in the opposite direction to that of its own). The third and final degree of freedom is the magnitude of the dipole moment, d, which is assumed to be equal for all dipoles in the system. The dipole unit vector is then given by,

$$\hat{\mathbf{d}}_{\mathbf{n}} = C_{\mathbf{n}}^{\pm}\left(\sin\varphi\cos\phi\mathbf{p}_1 + \sin\varphi\sin\phi\mathbf{p}_2 + \cos\varphi\mathbf{p}_3\right) \tag{5}$$

where $\mathbf{p}_1$, $\mathbf{p}_2$ and $\mathbf{p}_3$ is an arbitrary orthonormal reference frame and $C_{\mathbf{n}}^{\pm} = \pm 1$ is a corrugation term whose sign alternates for neighbouring sites. In the fully ordered case, $\alpha = 1$, the dipole vectors are simplified, $\hat{\mathbf{d}}_{\mathbf{n}} = C_{\mathbf{n}}^{\pm}\mathbf{p}_3$. Here, all dipoles are aligned to the same axis and neighbouring dipoles are pointed in opposite directions.

The lattice spacing is given by L, with an integer triplet lattice vector **n** and its equivalent unit vector, $\hat{\mathbf{n}}$, constructing a simple cubic lattice. The interaction energy between a charged particle and the lattice of permanent dipoles is given by,

$$e_{\mathbf{n}} = \frac{d}{\epsilon_r L^2}\frac{\hat{\mathbf{n}}\cdot\hat{\mathbf{d}}_{\mathbf{n}}}{|\mathbf{n}|^2}. \tag{6}$$

In evaluating the interaction energy of semi-ordered dipoles we follow the approach given by Young [37] for randomly ordered dipoles and introduce a term to account for the ordering. The variance of the site energies is given by evaluating two expected values, $\sigma^2_{\mathrm{corr}} = \langle E^2\rangle - \langle E\rangle^2$, where the average site energy is,

$$\langle E\rangle = \sum_{\mathbf{n}} \langle e_{\mathbf{n}}\rangle = 0, \tag{7}$$

since the arbitrary orthonormal reference frame for the dipoles is rotationally invariant and the underlying antiferromagnetic structure ensures that any dipole correlations average to zero. The second-order term is given by,

$$\langle E^2 \rangle = \sum_{\mathbf{n},\mathbf{n}'} \langle e_{\mathbf{n}} e_{\mathbf{n}'} \rangle. \tag{8}$$

This term consists of cross terms, $\mathbf{n} \neq \mathbf{n}'$ and diagonal terms, $\mathbf{n} = \mathbf{n}'$. The distribution of the diagonal terms, $\langle e_{\mathbf{n}}^2 \rangle$ is rotationally invariant since they are orientated against an arbitrary reference frame. When written in terms of the orthonormal frame of the lattice vectors, each component is equal and normalized. From this, we can state that the distribution of the dot product is 1/3 since there are 3 orthonormal vectors in the lattice. For a simple cubic lattice, $\sum_{\mathbf{n}} \mathbf{n}^{-4} = 16.5323...$ [38]. So, for the diagonal terms,

$$\sum_{\mathbf{n}} \langle e_{\mathbf{n}}^2 \rangle = \left(\frac{1}{\epsilon_r L^2} \right)^2 \cdot \frac{1}{3} \cdot 16.5323... = \left(d_0 \cdot d \right)^2, \tag{9}$$

where d_0 is the zero-order dipole constant,

$$d_0 = 2.3475 \cdot \frac{1}{\epsilon_r L^2}. \tag{10}$$

The distribution of the cross terms is zero for a randomly orientated set of dipole moments,[1] but is non-trivial for semi-ordered systems. For brevity, we collect the cross terms into,

$$X_\alpha = -\frac{1}{2.3475^2} \sum_{\mathbf{n},\mathbf{n}' \neq \mathbf{n}} \langle e_{\mathbf{n}} e_{\mathbf{n}'} \rangle. \tag{11}$$

So that we find,

$$\sigma_\alpha = \sqrt{1 - X_\alpha} \cdot \sigma_0. \tag{12}$$

Where σ_0 is the zero-order width of the DOS, given by,

$$\sigma_0 = d_0 \cdot d \tag{13}$$

3. Computational details

For each dipole magnitude and order configuration, we ran 22 simulations, each with uniquely generated dipole orientation and starting charge distribution with a carrier density of 10^{-5} nm^{-3}. Each simulation was performed on a cubic grid of 100 × 100 × 100 sites with a lattice spacing of $L = 1$ nm and ran for 10^6 time steps. To calculate the mobility we calculate the carrier flux in the direction of the field, Φ, defined as the difference of the cumulative count of *upfield* and *downfield* hopping events. The mobility is then given by,

$$\mu_h = \frac{1}{E_{\text{field}}} \cdot \frac{1}{N_{\text{charge}}} \cdot \frac{\Phi}{t_{\text{tot}}}, \tag{14}$$

where N_{charge} is the number of charged particles in the system, t_{tot} is the elapsed time and E_{field} is the field strength applied across the system. The time elapsed after each step, t_{step}, is determined by the sum of all calculated rates, k_{sum}, and a number chosen randomly from a uniform distribution between 0 and 1, ζ,

$$t_{\text{step}} = -\frac{\ln \zeta}{k_{\text{sum}}}. \tag{15}$$

The total elapsed time at any given step, t_{tot}, is given by the cumulative sum of all the time steps up to that point.

The mobility is reliably equilibrated after 2×10^5 steps. We take all data from subsequent steps to generate the average equilibrated mobility, μ_h. For the calculation of the correlated energy term, Eq. (4), we considered the effect of sites within $5\sqrt{3}L$ of the site of interest, as more distant sites do not contribute significantly. The inverse charge localization was set to $\gamma = 2$ nm^{-1}, the hopping attempt rate was set to $\omega_0 = 280 \times 10^{12}$ s^{-1}, the temperature was set to $T = 300$ K and the relative permittivity was set to $\epsilon_r = 3.0$. Finally, Table 1 lists the widths of the density of states used in the paper and their associated dipole magnitudes. The rates in Eq. (1) depend on the ratio of the energy differences between sites and the factor $k_B T$, so we evaluate noise widths corresponding to integer values of $k_B T$.

[1] Randomly orientated dipoles can be understood as independent variables, so $\langle e_{\mathbf{n}} e_{\mathbf{n}' \neq \mathbf{n}} \rangle = \langle e_{\mathbf{n}} \rangle \langle e_{\mathbf{n}' \neq \mathbf{n}} \rangle = 0$.

Table 1
Zero-order width of the density of states, σ_0, and the associated dipole magnitude, d.

σ_0 [$k_B T$]	1	2	3	4	5
σ_0 [eV]	0.026	0.052	0.078	0.103	0.129
d [D]	0.171	0.341	0.512	0.682	0.853

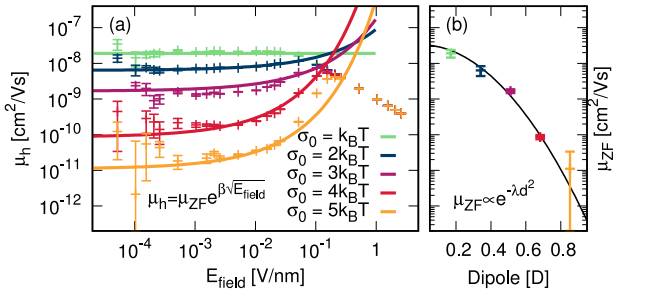

Fig. 1. (a) Charge mobility as a function of applied field for a range of dipole moments in the fully disordered configuration. The solid lines represent the fitted Poole–Frenkel-type empirical formula. (b) The zero-field mobility as a function of dipole moment, where the solid black line represents the fitted exponential function with $\lambda = 12.5 \pm 0.5$.

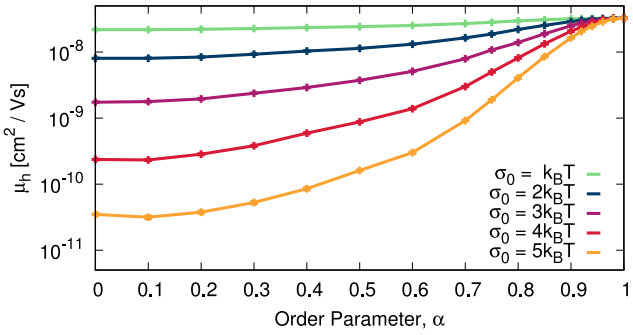

Fig. 2. Mobility at $E_{\text{field}} = 0.01$ V/nm as a function of the order parameter for systems with a range of dipole moments.

4. Results

In the fully disordered systems, with $\alpha = 0$, we see Poole–Frenkel behaviour [33] ($\mu_h \propto e^{\beta\sqrt{E_{\text{Field}}}}$) for applied electric fields below 1 V/nm. Fig. 1(a) shows the calculated mobilities of the fully disordered systems for $\sigma_0 = k_B T$, $2k_B T$, $3k_B T$, $4k_B T$ and $5k_B T$, along with a fitted Poole–Frenkel-type empirical formula. Fig. 1(b) shows the extrapolated zero-field mobility as a function of the dipole magnitude. Here, we see the expected exponential decay of the zero-field mobility with the square of the dipole ($\mu_{\text{ZT}} \propto e^{\lambda d^2}$). In this case, even for a modest dipole, the mobility is reduced by orders of magnitude.

Fig. 2 shows a plot of mobility against dipole moment for a series of systems with increasing dipole moment as a function of the order parameters, α. In the zero-order case, $\alpha = 0$, where the dipole orientations are distributed randomly, we observe a rapid decay in the mobility as the dipole moment is increased, consistent with Fig. 1(b) and Refs. [11,12], which is directly related to an increased energetic disorder associated with E^{corr}. With the increased ordering of the dipoles, we see a dramatic increase in mobility, culminating in the fully-ordered systems, which all have the same mobility, *i.e.* the effect of the

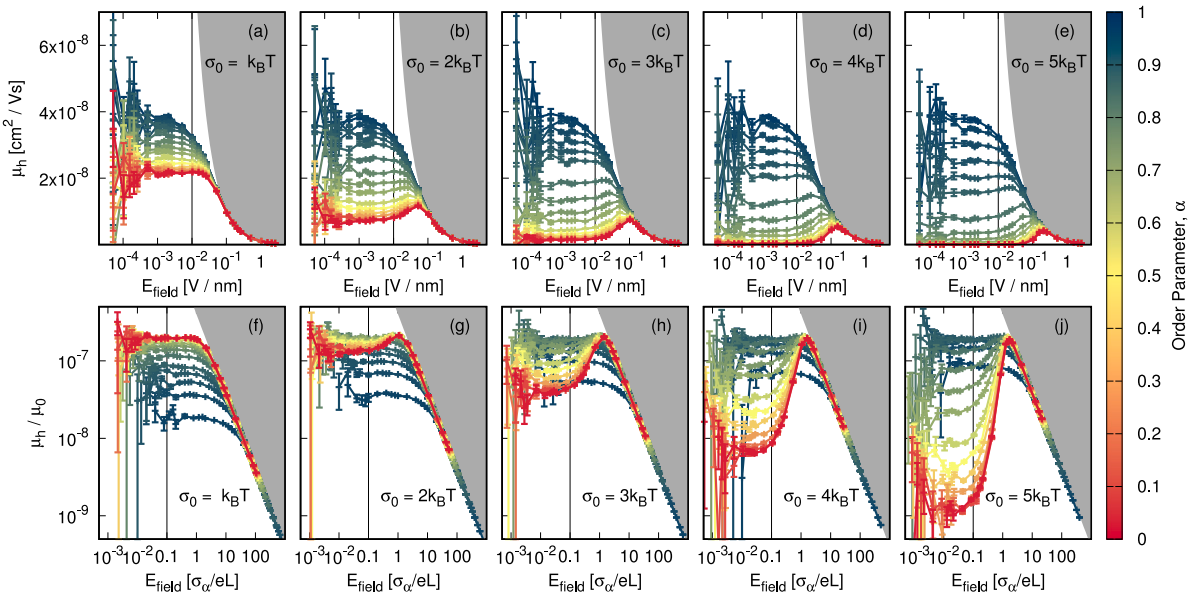

Fig. 3. (a–e) Mobility as a function of electric field and the order parameter for the system with a dipole moment corresponding to a zero-order width of the density of states which are $\sigma_0 = k_BT$, $2k_BT$, $3k_BT$, $4k_BT$ and $5k_BT$ respectively. (f–j) Normalized mobility as a function of electric field and the order parameter for the system with a dipole moment corresponding to a zero-order width of the density of states of $\sigma_0 = k_BT$, $2k_BT$, $3k_BT$, $4k_BT$ and $5k_BT$ respectively. For all cases, the grey-shaded region denotes the saturation point and the vertical line denotes the value for the electric field at which the data for Figs. 2 and 4 are extracted.

dipole moment is removed. This is expected behaviour, since the cross-term parameter, X_α is expected to tend towards one in the fully ordered case so that the width, σ_α will be zero.

Fig. 3(a–e) shows the dependence of mobility on the electric field for the full range of α, *i.e.* the order parameter in the system, and for $\sigma_0 = k_BT$, $2k_BT$, $3k_BT$, $4k_BT$ and $5k_BT$ respectively. In general, the mobility is maximized when the field strength is tuned such that it and the dipole interaction term contribute an equal amount to the energy term in the rate equation (Eq. (1)).[2] This point occurs at $E_{\text{field}}^{\max} = 2\times(\sigma_0 - k_BT)/eL$. At a higher field strength, the mobility is inhibited by the saturation point, the point at which the electric field is large enough that *upfield* hopping events become vanishingly unlikely. For clarity, the region beyond the saturation point is shaded in grey. At the mobility peak, the higher-ordered systems, $\alpha > 0.6$, have larger mobilities as expected. In addition, this peak is broader in the low-dipole systems as the effect of the dipole moment on the energetic landscape is significantly lower and, thus, a lower field is required to overcome the energy barrier. Finally, at lower fields, the mobility decreases as the field decreases because the field is insufficient to make an appreciable difference to the choice for hopping events in the KMC algorithm. This effect is exacerbated by higher dipole magnitude and low order.

So far, the effect of the dipole moment has been understood in terms of its influence on the width of the density of states (i.e. the dipole energy contribution has been mapped onto an uncorrelated energy distribution randomly drawn from a Gaussian density of states with a width of the density of states, σ_α), but further analysis will show that this does not provide the complete picture. For all the systems, we evaluate the width of the density of states numerically and use it to define $\mu_0 = L^2\omega_0/\sigma_\alpha$, which is the prefactor to the zero-field approximation of the charge mobility in the Boltzmann regime,

$$\mu(T) = c_1\mu_0 e^{-c_2(\sigma_\alpha/k_BT)^2}. \tag{16}$$

Here, c_1 and c_2 are empirical parameters that may be determined by fitting to numerical data. For our purpose, however, μ_0 may be viewed as a normalization parameter incorporating the effects of a global

[2] Assuming that the contribution of the coulomb term is generally not correlated with respect to the direction of the electric field.

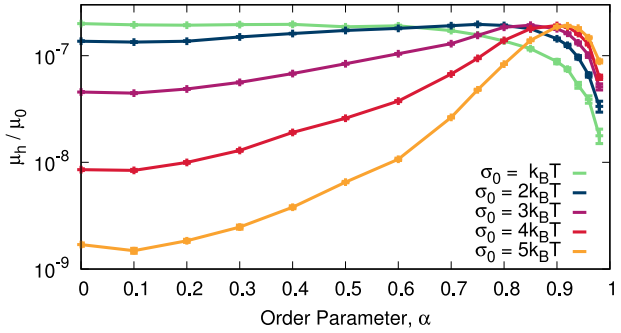

Fig. 4. Normalized mobility at $E_{\text{field}} = 0.1\times\sigma_\alpha/eL$ as a function of the order parameter for systems with a range of dipole moments.

random noise of width σ_α. Figs. 3(f–j) show the mobilities of Figs. 3(a–e) in units of μ_0. If the effect of the dipole moment can be completely described by the width of the density of states, we would expect the *normalized* mobilities to be constant. We see, instead, that the effect of the ordering parameter, α, is different for each value of the dipole moment. When $\sigma_0 = k_BT$, the order parameter is less beneficial to the mobility than one would expect, because the higher ordered systems (blue–green, $\alpha > 0.7$) have normalized mobilities an order of magnitude smaller than the low-ordered systems (yellow-red, $\alpha < 0.3$). This is due to the $1/\sigma_\alpha$ character of the mobility parameter μ_0 meaning that when the system is highly ordered, the width of the density of states tends to zero and so the mobility parameter becomes large. This behaviour has a larger effect on the low-dipole system.

For a field strength lower than $E_{\text{field}}^{\max}$, we see that the highest normalized mobilities occur in lower-order systems. The precise level of dipole ordering needed to maximize the normalized mobility depends on the dipole magnitude and the applied electric field, but typically occurs within the range $0.7 < \alpha < 0.9$. To further explore this, in Fig. 4 the normalized mobility is plotted for an arbitrary field strength less than $E_{\text{field}}^{\max}$, $E_{\text{field}} = 0.1\times\sigma_\alpha/eL$. The maximum in the normalized mobility occurs between α=0.7–0.95 for systems with $\sigma_0 > k_BT$. For higher order parameters, the width of the density of states tends to zero and μ_0 becomes large. In the lower order cases, the normalized

mobility decreases as disorder increases, with this effect being more significant in higher dipole systems. Notably, the mobility maximum occurs at a higher order parameter for systems with a larger dipole. Since the normalization factor, μ_0, includes a global random noise of width σ_α, the maximum in normalized mobilities for intermediate order parameters suggests that non-trivial localized effects are contributing to the higher mobilities.

To further investigate the effect of the dipole moment, we analysed the cumulative charge population (CCP) of each site, defined as the total number of charged particles that have hopped onto a given site within the simulation, all of which are performed after 10^6 time steps. This metric indicates the energetic environment experienced by the charged particles, as energetically accessible sites will exhibit a larger CCP. Fig. 5(a) shows the proportion of sites with a non-zero CCP as a function of the order parameter for each dipole magnitude studied. In the fully ordered system, the CCP is distributed over a large proportion of the system (≥50%), since the effect of the dipole interactions is negated by the ordering, all the sites are energetically accessible. When the order parameter is reduced, we observe a decrease in the proportion of sites with non-zero CCP, which is compounded by an increase in the dipole moment. The effect of the dipole is to reduce the number of energetically accessible sites for any given charged particle producing more localized transport. An example of the CCP in a fully disordered system for $\sigma_0 = 4k_BT$ is shown in Fig. 5(b). This shows large regions in the system that have zero population throughout the simulation. Whereas, Fig. 5(c) shows an example of the CCP for a fully ordered system indicating the CCP is effectively homogeneous. From this perspective, the rapid decrease in mobility with an increasing dipole is easy to understand: for the cases where there is zero order, increasing the dipole moment increases the energy cost for a large number of hopping events and effectively forces the charged particles onto a smaller proportion of the system. This can lead to more circuitous *downfield* paths and, in the case of energetic dead-ends, the increased influence of specific, energetically unfavourable hopping events. All of which reduce mobility. The fact that the particles are forced into a smaller region will also affect the coulomb term, which depends strongly on the local population density. This is a significant effect in multilayered devices, where injection barriers can depend strongly on coulomb correlation [39]. In addition to this, the higher energy cost of the hopping events leads to a longer time delay between events, also reducing mobility. When dipole ordering is present, the energy cost is reduced and so simultaneously, more of the system is available and the hopping events occur more rapidly.

However, this also demonstrates the origin of the breakdown of the normalization parameter, μ_0, which incorporates the effects of a global random noise of width σ_α. Indeed, as the noise width increases, local interactions between the dipole moments play a stronger role in determining the overall mobility.

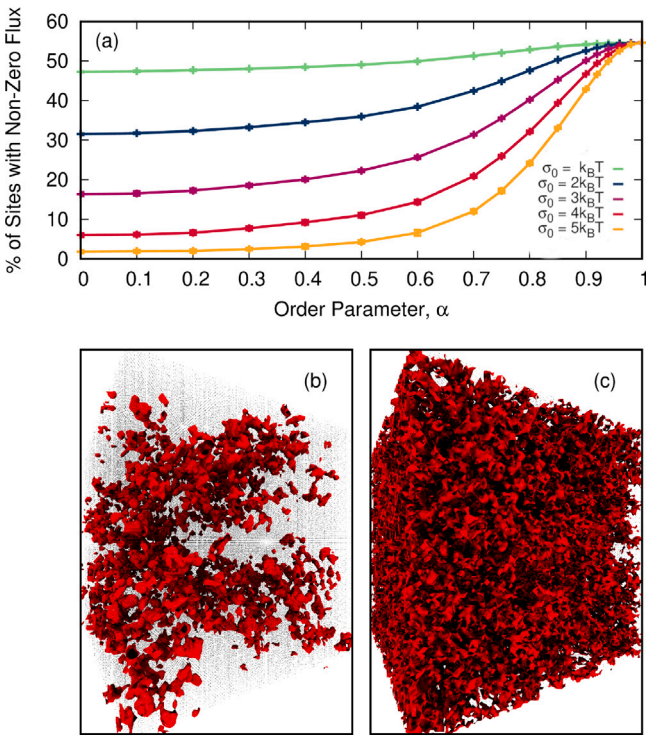

Fig. 5. (a) Proportion of the sites in the system that have been populated by a charge at least once throughout the simulation against the order parameter for a range of dipole magnitudes. (b, c) Cumulative charge population density over the system for a dipole moment corresponding to a zero-order width of the density of states of $\sigma_0 = 4k_BT$ with an order parameter of 0.0 (b) and 1.0 (c).

5. Discussion and conclusions

In this work, we have used a KMC algorithm to study the effect of dipole ordering on the hole mobility of organic molecular semiconductors. We observe, consistent with previous work, that the presence of significant dipole–dipole interaction creates an energetically unfavourable environment for charge transport through the system for a case where the dipole moments are random, *i.e.* in an amorphous thin film. Here, the charged particles are effectively restricted to localized regions within the system and the mobility is significantly reduced.

As order within the film is increased, which can arise from an increase in dipole–dipole interactions, a significant reduction in the width of the density of states of the correlated disorder is observed which allows more of the system to be accessible to any given charge. However, the present analysis also demonstrates a non-trivial behaviour of mobility in terms of the dipole moment. Indeed, the random noise of width σ_α is a global measure of the system and as the dipole moment increases local interactions between the dipole moments are more significant, producing preferred localized routes for the charges through the thin film, as demonstrated by the CCP. Failure to consider this local order may result in an overestimation of the effect of the dipole moment.

Despite this, throughout this work, we observe a significant reduction in mobility as a function of the magnitude of the dipole moment. The dipole ordering increase can have a significant impact in offsetting this and enhancing the charge-carrier mobility. However, the magnitude of the ordering required to completely counteract this is significant and unlikely to be achieved in solution-processed films. Consequently, it would appear that recently reported materials exhibiting high mobility and also a large permanent dipole moment [30,31], exhibit this mobility despite the dipole moment rather than because of it. While it has been proposed that the large dipole moment promotes close packing leading to a high density in the films and an increase in the coupling between the individual units, this would also significantly increase the correlated disorder, as shown in Eq. (5). This does not rule out the effect of other intramolecular interactions, such as hydrogen bonding as recently proposed by Mimaite et al. [40], however assessment of these effects would require atomistic simulations of the thin film which will be the focus of future work.

Declaration of competing interest

The authors declare that they have no known competing financial interests or personal relationships that could have appeared to influence the work reported in this paper.

Data availability

Data will be made available on request.

Acknowledgements

The research described in this paper was funded by the EPSRC, United Kingdom (Grant Nos. EP/R021503/1, EP/T022442/1, and EP/S023836/1). This research made use of the Rocket High-Performance Computing service at Newcastle University.

References

[1] C.W. Tang, S.A. VanSlyke, Organic electroluminescent diodes, Appl. Phys. Lett. 51 (12) (1987) 913–915.
[2] C. Deibel, V. Dyakonov, Polymer–fullerene bulk heterojunction solar cells, Rep. Progr. Phys. 73 (9) (2010) 096401.
[3] S. Allard, M. Forster, B. Souharce, H. Thiem, U. Scherf, Organic semiconductors for solution-processable field-effect transistors (OFETs), Angew. Chem. Int. Ed. 47 (22) (2008) 4070–4098.
[4] H.S. Jung, N.-G. Park, Perovskite solar cells: From materials to devices, Small 11 (1) (2015) 10–25.
[5] M.L. Petrus, J. Schlipf, C. Li, T.P. Gujar, N. Giesbrecht, P. Müller-Buschbaum, M. Thelakkat, T. Bein, S. Hüttner, P. Docampo, Capturing the sun: A review of the challenges and perspectives of Perovskite solar cells, Adv. Energy Mater. 7 (16) (2017) 1700264.
[6] J. Kwiatkowski, J. Nelson, H. Li, J. Brèdas, W. Wenzel, C. Lennartz, Simulating charge transport in tris (8-hydroxyquinoline) aluminium (Alq 3), Phys. Chem. Chem. Phys. 10 (14) (2008) 1852–1858.
[7] S.M. Ryno, C. Risko, J.-L. Brèdas, Impact of molecular packing on electronic polarization in organic crystals: The case of pentacene vs TIPS-pentacene, J. Am. Chem. Soc. 136 (17) (2014) 6421–6427.
[8] P. Friederich, V. Meded, A. Poschlad, T. Neumann, V. Rodin, V. Stehr, F. Symalla, D. Danilov, G. Lüdemann, R.F. Fink, et al., Molecular origin of the charge carrier mobility in small molecule organic semiconductors, Adv. Funct. Mater. 26 (31) (2016) 5757–5763.
[9] R.H. Young, T.-M. Kung, J.A. Sinicropi, N.G. Rule, J.J. Fitzgerald, J.E. Eilers, C.H. Chen, N.W. Boaz, Effect of group and net dipole moments on electron transport in molecularly doped polymers, J. Phys. Chem. 100 (45) (1996) 17923–17930.
[10] R.H. Young, J.J. Fitzgerald, Effect of polar additives on charge transport in a molecularly doped polymer: Survey of various additives, J. Chem. Phys. 102 (5) (1995) 2209–2221.
[11] R.H. Young, J.J. Fitzgerald, Dipole moments of hole-transporting materials and their influence on hole mobility in molecularly doped polymers, J. Phys. Chem. 99 (12) (1995) 4230–4240.
[12] R.H. Young, J.A. Sinicropi, J.J. Fitzgerald, Dipole moments, energetic disorder, and charge transport in molecularly doped polymers, J. Phys. Chem. 99 (23) (1995) 9497–9506.
[13] H. Bässler, Localized states and electronic transport in single component organic solids with diagonal disorder, Phys. Status Solidi (B) 107 (1) (1981) 9–54.
[14] A. Dieckmann, H. Bässler, P. Borsenberger, An assessment of the role of dipoles on the density-of-states function of disordered molecular solids, J. Chem. Phys. 99 (10) (1993) 8136–8141.
[15] P. Borsenberger, H. Bässler, Concerning the role of dipolar disorder on charge transport in molecularly doped polymers, J. Chem. Phys. 95 (7) (1991) 5327–5331.
[16] M. Baldo, Z. Soos, S. Forrest, Local order in amorphous organic molecular thin films, Chem. Phys. Lett. 347 (4–6) (2001) 297–303.
[17] R.L. Martin, J.D. Kress, I. Campbell, D. Smith, Molecular and solid-state properties of tris-(8-hydroxyquinolate)-aluminum, Phys. Rev. B 61 (23) (2000) 15804.
[18] D.H. Dunlap, P.E. Parris, V.M. Kenkre, Charge-dipole model for the universal field dependence of mobilities in molecularly doped polymers, Phys. Rev. Lett. 77 (3) (1996) 542.
[19] S.V. Novikov, D.H. Dunlap, V.M. Kenkre, P.E. Parris, A.V. Vannikov, Essential role of correlations in governing charge transport in disordered organic materials, Phys. Rev. Lett. 81 (20) (1998) 4472.
[20] M. Tanaka, H. Noda, H. Nakanotani, C. Adachi, Molecular orientation of disk-shaped small molecules exhibiting thermally activated delayed fluorescence in host–guest films, Appl. Phys. Lett. 116 (2) (2020) 023302.
[21] L. Jäger, T.D. Schmidt, W. Brütting, Manipulation and control of the interfacial polarization in organic light-emitting diodes by dipolar doping, AIP Adv. 6 (9) (2016) 095220.
[22] Y. Noguchi, Y. Miyazaki, Y. Tanaka, N. Sato, Y. Nakayama, T.D. Schmidt, W. Brütting, H. Ishii, Charge accumulation at organic semiconductor interfaces due to a permanent dipole moment and its orientational order in bilayer devices, J. Appl. Phys. 111 (11) (2012) 114508.
[23] K. Bagchi, N.E. Jackson, A. Gujral, C. Huang, M.F. Toney, L. Yu, J.J. De Pablo, M. Ediger, Origin of anisotropic molecular packing in vapor-deposited Alq3 glasses, J. Phys. Chem. Lett. 10 (2) (2018) 164–170.
[24] K. Bagchi, M. Ediger, Controlling structure and properties of vapor-deposited glasses of organic semiconductors: Recent advances and challenges, J. Phys. Chem. Lett. 11 (17) (2020) 6935–6945.
[25] L.W. Antony, N.E. Jackson, I. Lyubimov, V. Vishwanath, M.D. Ediger, J.J. De Pablo, Influence of vapor deposition on structural and charge transport properties of ethylbenzene films, ACS Central Sci. 3 (5) (2017) 415–424.
[26] E. Ito, Y. Washizu, N. Hayashi, H. Ishii, N. Matsuie, K. Tsuboi, Y. Ouchi, Y. Harima, K. Yamashita, K. Seki, Spontaneous buildup of giant surface potential by vacuum deposition of Alq3 and its removal by visible light irradiation, J. Appl. Phys. 92 (12) (2002) 7306–7310.
[27] P. Friederich, V. Rodin, F. Von Wrochem, W. Wenzel, Built-in potentials induced by molecular order in amorphous organic thin films, ACS Appl. Mater. Interfaces 10 (2) (2018) 1881–1887.
[28] T. Lee, A.V. Sanzogni, P.L. Burn, A.E. Mark, Evolution and morphology of thin films formed by solvent evaporation: An organic semiconductor case study, ACS Appl. Mater. Interfaces 12 (36) (2020) 40548–40557.
[29] A.S. Gertsen, M.K. Sørensen, J.W. Andreasen, Nanostructure of organic semiconductor thin films: Molecular dynamics modeling with solvent evaporation, Phys. Rev. Mater. 4 (7) (2020) 075405.
[30] M.L. Petrus, K. Schutt, M.T. Sirtl, E.M. Hutter, A.C. Closs, J.M. Ball, J.C. Bijleveld, A. Petrozza, T. Bein, T.J. Dingemans, et al., New generation hole transporting materials for Perovskite solar cells: Amide-based small-molecules with nonconjugated backbones, Adv. Energy Mater. 8 (32) (2018) 1801605.
[31] M.L. Petrus, A. Music, A.C. Closs, J.C. Bijleveld, M.T. Sirtl, Y. Hu, T.J. Dingemans, T. Bein, P. Docampo, Design rules for the preparation of low-cost hole transporting materials for perovskite solar cells with moisture barrier properties, J. Mater. Chem. A 5 (48) (2017) 25200–25210.
[32] L. Pautmeier, R. Richert, H. Bässler, Poole-Frenkel behavior of charge transport in organic solids with off-diagonal disorder studied by Monte Carlo simulation, Synth. Met. 37 (1–3) (1990) 271–281.
[33] H. Bässler, Charge transport in disordered organic photoconductors. a Monte Carlo simulation study, Phys. Status Solidi B (Basic Research);(Germany) 175 (1) (1993).
[34] W. Pasveer, J. Cottaar, C. Tanase, R. Coehoorn, P. Bobbert, P. Blom, D. De Leeuw, M. Michels, Unified description of charge-carrier mobilities in disordered semiconducting polymers, Phys. Rev. Lett. 94 (20) (2005) 206601.
[35] M. Bouhassoune, S. Van Mensfoort, P. Bobbert, R. Coehoorn, Carrier-density and field-dependent charge-carrier mobility in organic semiconductors with correlated Gaussian disorder, Org. Electron. 10 (3) (2009) 437–445.
[36] D. Balzer, T.J. Smolders, D. Blyth, S.N. Hood, I. Kassal, Delocalised kinetic Monte Carlo for simulating delocalisation-enhanced charge and exciton transport in disordered materials, Chem. Sci. 12 (6) (2021) 2276–2285.
[37] R.H. Young, Dipolar lattice model of disorder in random media analytical evaluation of the gaussian disorder model, Philos. Mag. B 72 (4) (1995) 435–457.
[38] R.D. Misra, On the stability of crystal lattices. II, in: Mathematical Proceedings of the Cambridge Philosophical Society, Vol. 36, no. 2, Cambridge University Press, 1940, pp. 173–182.
[39] F. Liu, H. van Eersel, B. Xu, J.G. Wilbers, M.P. de Jong, W.G. van der Wiel, P.A. Bobbert, R. Coehoorn, Effect of Coulomb correlation on charge transport in disordered organic semiconductors, Phys. Rev. B 96 (20) (2017) 205203.
[40] V. Mimaite, J.V. Grazulevicius, R. Laurinaviciute, D. Volyniuk, V. Jankauskas, G. Sini, Can hydrogen bonds improve the hole-mobility in amorphous organic semiconductors? Experimental and theoretical insights, J. Mater. Chem. C 3 (44) (2015) 11660–11674.